Reversible chiral switching of bis(phthalocyaninato) terbium(III) on a metal surface

Ying-Shuang Fu [1,*], *Jörg Schwöbel* [1], *Saw-Wai Hla* [2], *Andrew Dilullo* [2], *Germar Hoffmann* [1], *Svetlana Klyatskaya* [3], *Mario Ruben* [3,4], *and Roland Wiesendanger* [1]

1. Institute of Applied Physics, Hamburg University, 20355 Hamburg, Germany
2. Department of Physics and Astronomy, Ohio University, Athens, Ohio 45701, USA
3. Institute of Nanotechnology, Karlsruhe Institute of Technology, 76344 Eggenstein-Leopoldshafen, Germany
4. IPCMS, Université de Strasbourg, 67034 Strasbourg, France

*To whom correspondence should be addressed. E-mail: yfu@physnet.uni-hamburg.de

ABSTRACT We demonstrate a reversible chiral switching of bis(phthalocyaninato) terbium(III) molecules on an Ir(111) surface by low temperature scanning tunneling microscopy. With an azimuthal rotation of its upper phthalocyanine ligand, the molecule can be switched between a chiral and an achiral configuration actuated by respective inelastic electron tunneling and local current heating. Moreover, the molecular chiral configuration can be interchanged between left and right handedness during the switching manipulations, thereby opening up potential nanotechnological applications.

KEYWORDS: Molecule Chirality, Molecule Switch, Scanning Tunneling Microscopy, Molecule Manipulation, $TbPc_2$.

Molecular switches interconvert between bistable states and could function as potential storage bits for building molecule-based devices[1]. With scanning tunneling microscopy (STM), various molecular switches supported on surfaces can be studied at the single molecule level[2-15]. Most molecular switches operate by changing conformation[2-11] although other forms of operations like electron charging[11-14] or bond formation[15] have also been demonstrated recently. Chirality, on the other hand, is of fundamental importance in biological systems and also has technological significance for asymmetric heterogeneous catalysis. If one could control the chirality within a single molecule, its physical properties (e.g. photophysics) as well as functionalities (e.g. catalytic activities) could also be controlled. STM offers a unique tool to investigate molecular chirality, ranging from supramolecular organization[16, 17] to chirality manipulation of single adsorbates[18, 19]. Here we demonstrate a molecular switch using bis(phthalocyaninato) terbium(III) ($TbPc_2$) molecules adsorbed on Ir(111), where a chirality change is explicitly manifested,.

$TbPc_2$ is composed of two organic phthalocyanine (Pc) ligands with a terbium (III) metal ion sandwiched in between (Fig. 1a). As a free molecule, its two Pc ligands have a relative staggering angle of 45° [20]. Due to its single molecule magnet behavior originating from the lanthanide ion, the double-decker class molecule has attracted intense research interests[21-27]. It was shown recently that the spin state of $TbPc_2$ on Au(111) can be modified with molecular switching[25], where the molecules studied were embedded in a self-assembled monolayer film.

The experiments were performed with a home-made low temperature STM[28] at 6 K in ultra-high vacuum. The Ir(111) substrate was cleaned by Ar^+ ion sputtering at 800 V and then flashing to 1200 °C for 2 minutes. Then the sample was annealed under an oxygen pressure of

8.0×10^{-7} mbar followed by flashing cycles to remove carbon impurities. $TbPc_2$ molecules were thermally sublimed *in situ* onto the Ir(111) substrate from a home-built ceramic cell evaporator held at ~700 K. During deposition, the substrate was kept either at room temperature or at ~100 K. An electron beam heated tungsten tip was used as the STM probe. The dI/dV-V scanning tunneling spectroscopy (STS) data were acquired by a lock-in detection of the tunneling current with a modulation voltage of 1777 Hz superimposed to the sample voltage.

STM images show a random distribution of individual $TbPc_2$ molecules on the Ir(111) surface deposited at room temperature (Fig S1). All molecules adopt a face-on configuration, i.e., with one Pc ligand facing the surface. When the STM images are taken with a bias voltage of ~ 1.7 V, the molecules appear with *asymmetric* shapes (Fig 1b and Fig S1b) with distinctive intensity contrast between their two pairs of opposite pyrrole rings. However, they appear as very similar 4-lobed structures (Fig. 1c and Fig S1a) when imaged with lower voltages. In previous studies of $TbPc_2$ molecules on metal surfaces, a mirror *symmetric*, thereby *achiral*, 8-lobed structure is commonly observed where the top and bottom Pc ligands are staggered 45° to each other[22, 23]. Indeed, we are able to switch the asymmetric molecules in Fig. 1b to the achiral 8-lobed structure (Fig. 1d and Fig. 1h) using an STM manipulation scheme. The two molecules in Fig. 1b, we denote as 'L' and 'R' type, respectively, cannot be superposed on their own mirror images, but are mirror images of each other. Thus they are *chiral* and represent two enantiomers with [1-10] surface direction (Fig. 1e) as their mirror-symmetry axis. Careful analysis reveals that the two molecules in Fig. 1c are slightly misaligned with respect to [1-10]. The marked principal axes of the molecules indicate a misalignment angle of +4° for the top molecule (R) and -4° for the lower one (L) (Fig. 1f, and 1h). We define the molecule possessing the - (+) 4° misalignment, i.e. L (R) type, as left

(right)-handed. After the switching the misalignment disappears, and the molecular principal axes are then aligned with the substrate [1-10] direction (Fig. 1d, and 1h).

There are two possible rotational scenarios to account for the 4° misalignment and the observed chirality: a whole-rotational configuration, where the molecule keeps the 45° staggering angle between its two Pcs and rotates by 4° with respect to the crystallographic direction of Ir(111) as a whole; or a relative-rotational configuration, in which the lower Pc stays aligned with the substrate leaving the upper Pc rotated by 4°. To differentiate these two scenarios, we performed STM lateral manipulations to the molecule. The upper Pc ligand is removed from the molecule, leaving the lower single-decker at the original place. The remaining single-decker[29] aligns with the substrate crystallographic direction and is staggered 45° relative to the upper one (Fig. 1g). This demonstrates that the lower Pc binds tightly to the substrate and the relative-rotational configuration is adopted by the chiral molecule. Moreover, the azimuthal rotational motion of the double-decker complex has been explored in several studies[25, 30, 31], which support the above arguments. It can thus be concluded that the molecular switching event is associated with a relative azimuthal rotation between the upper Pc and the surface-immobilized lower Pc (Fig. 1h) [32, 33]. Due to the three dimensional structure of $TbPc_2$, the relative-rotation lifts its mirror symmetry, rendering it a chiral motif.

To switch a molecule, a voltage pulse is applied to the center of its top Pc ligand with opened feedback loop. During this process, the tunneling current is recorded as a function of time. An abrupt change in the tunneling current is associated with a switching event. A sequence of STM induced molecular switching events is presented in Fig. 2. When a +2 V voltage pulse is applied to the right molecule in Fig. 2a, it switches from the chiral 4-lobed to the achiral 8-

lobed state (Fig. 2b). The corresponding tunneling current signal shows an abrupt change in magnitude upon the switching (Fig. 2e)[8,34]. The molecule can be switched with negative voltage pulses as well. A -2 V pulse (Fig. 2e) switches the left molecule in Fig. 2b to the achiral 8-lobed structure (Fig. 2c). For the reverse switching from the achiral 8-lobed to the chiral 4-lobed state, a different STM manipulation scheme is used: With a fixed bias voltage of 50 mV, the tip is approached to the center of the right molecule in Fig. 2c and then retracted to its original position after 0.1 seconds[35]. During the tip approach, the tunneling current increases exponentially (Fig. 2f). At ~700 nA, a sudden drop of the current occurs (marked with a red arrow), denoting the switching of the molecule. The reverse switching of the left molecule is confirmed by STM imaging in Fig. 2d, where it now shows the restored chiral 4-lobed structure. The success rate of this process is ~5%, as the molecule often decomposes due to the high current. Note that with the tip approaching laterally as in our decomplexation experiment, a much lower current of about 5 nA is sufficient to decompose the molecule.

To understand the mechanisms of switching, STS measurements are performed by positioning the STM tip above the center of a chiral molecule. As shown in Fig 3a, when the sample bias is ramped from -1.5 V to +2.5 V, the dI/dV signal is featureless until it reaches +1.5 V where its intensity rapidly increases. Thus, we assign +1.5 V as the onset of the lowest unoccupied molecular orbital (LUMO) of the chiral state. Before reaching a peak maximum, the conductance abruptly drops at ~ +2 V due to the molecular switching to the achiral state. When the bias voltage is ramped back, the dI/dV curve follows a distinctly different trajectory of the newly switched achiral state. Now two prominent peaks appear at +1.2 V and -1.1 V, which are ascribed to the LUMO and the highest occupied molecular orbital (HOMO) of the achiral state, respectively. Similarly, to switch the chiral molecule using a negative bias

voltage, the bias is ramped from +1.5 V to -2.5 V. The recorded dI/dV curve is also featureless until -1.8 V where an increase in conductance occurs, which is assigned as the HOMO of the chiral state. At ~ -2 V, the molecule switches to the achiral state, and when the bias is ramped back, the previously observed HOMO and LUMO peaks of the achiral state show up again (Fig. 3a).

In light of the explicit overlap between the manifested conductance jump and a molecular state, we attribute the switching event from the chiral to achiral state to be induced by inelastic electron tunneling (IET)[2, 6]. In an IET process, the energy of tunneling electrons is transferred to the molecule via a temporary electron attachment to the molecule and the subsequent vibrational relaxiations[8,34]. When the transferred energy is large enough to overcome the energy barrier of an azimuthal rotation of the molecule's upper Pc, the switching event occurs. An IET-induced switching process does not necessarily require a resonant tunneling condition. However, in the case of off-resonance tunneling, the tunneling electron's residing time on the molecule exponentially decreases with reduced electron energy to the resonance ion state, thereby dramatically diminishing the probability of switching[3, 6]. To rule out other possible switching mechanisms, we investigated the tip-sample distance dependence of the threshold switching bias, which gives an almost constant value (Fig. S2). This observation demonstrates that the switching process is not driven by the electrical field or a thermal process, because it is independent of the electric field [2] and the power of tunneling electrons.

We found that $TbPc_2$ molecules deposited at a low substrate temperature of ~100 K all show the achiral 8-lobed configuration (Fig. S3). After annealing the sample to room temperature,

all the molecules appear in the chiral configuration indicating that a thermally assisted process can switch the molecules from the achiral to the chiral state. Therefore, for the reverse switching shown in Fig. 2f, the process is very likely triggered by tunneling-electron-generated local heating[36], similar to the thermal switching process because of the high current (~700 nA)[37]. It is noted that a low bias voltage (50 mV) was used in Fig. 2f to ensure the tunneling electrons are of low energy, preventing the molecule from switching back to the achiral state via IET. A low negative bias voltage of -50 mV has also been successfully employed to switch the molecule from an achiral to a chiral state, substantiating the reversal switching may be caused merely by a local heating effect as it is insensitive to bias polarity.

Next, we directly visualize the spatial distribution of the molecule's frontier orbitals via dI/dV spectroscopic mapping. Fig. 3b shows two $TbPc_2$ molecules of different states. Their dI/dV maps are presented in Fig. 3c: At -1.0 V (+1.0 V) where the HOMO (LUMO) of the achiral molecule is located, an intense molecular orbital with 8 well (less) separated lobes is resolved on the ligand. This is in agreement with previous reports of the same molecule adsorbed on Cu(111)[22], and can be correspondingly attributed to the π orbital of the upper Pc. The intensity of the chiral molecule is low in accordance with its off resonance tunneling condition. While at -1.8 V (+1.7 V) where the tail of the chiral molecule's HOMO (LUMO) resides, an intense molecule orbital is observed, the electronic signature of the achiral molecule fades out. Remarkably, the LUMO of the chiral molecule exhibits a distortion away from its square shape, with prominent intensity contrast between its two pairs of opposite lobes. This evidences that the structural chirality is transformed into a chiral electronic structure, which is responsible for the clear chirality expression from the topographic images taken at +1.7 V in Fig 1b. The HOMO of the chiral molecule shows 4 bright lobes[38] staggered on top of a square-shaped state, which may originate from its lower and upper Pc ligand

respectively, as judged from their orientations relative to the molecule. Interestingly, the mirror axis of the 4 bright lobes (marked with a black line) aligns with the substrate crystallographic direction, and rotates by about 4° relative to the molecule's principal axis (marked with a green line), substantiating the proposed relative-rotational configuration of the chiral molecule.

It is computationally challenging to accurately model the adsorption configuration and electronic structure of $TbPc_2$ adsorbed on the Ir(111) substrate due to its large size. Nevertheless, recently reported density functional theory calculations performed for a free molecule could give some insight into our spectroscopic features. The conductance mapping of the 8-lobed molecule's ligand frontier orbitals matches those of an isolated $[TbPc_2]^-$ as calculated in Ref. 21. An azimuthal rotation between the two Pc rings changes their mutual coupling strength, and consequently shifts the frontier orbitals of $TbPc_2$[25]. According to Ref. 19, the HOMO-LUMO gap of $[TbPc_2]^-$ becomes wider with a small azimuthal rotational angle between the two Pcs. This qualitatively reproduces the trend of our observation: The HOMO-LUMO gap changes from ~2 V of the achiral 8-lobed state to ~4 V of the chiral 4-lobed state.

We further demonstrate that the chiral $TbPc_2$ can be switched between its two enantiomer states by STM. Because the azimuthal rotation of the molecule's upper Pc can be either clockwise or counter-clockwise when switching, this provides the feasibility of changing the handedness of the chiral molecule with switching manipulations. Fig. 4a shows a molecule with right-handedness as revealed from the STM imaging at 1.7 V. When imaging at a sample bias of -2.5 V, the molecule is switched to the achiral state during scanning, leaving an abrupt

change in the scanning line (Fig. 4b). In this way, the chiral molecules within the scanning range can be switched with certainty to the achiral state in a more efficient manner. After switching back to the chiral state, the molecule now possesses left-handedness (Fig. 4c).

In summary, we have demonstrated a molecular switch based on a process of reversible chirality change. By means of respective inelastic electron tunneling and local current heating, the $TbPc_2$ molecule can be switched among left and right-handed configurations and that of an achiral configuration. In view of the intricate correlation between magnetism and structure, the chiral switching of the molecule paves the way for future studies on how the magnetic behavior of molecular magnets evolves with molecular switching at a single molecule level by spin-polarized STM[39]. Additionally, the double-decker single molecule magnet can be prepared macroscopically in one of the bistable states simply by deposition at different substrate temperatures, which allows using ensemble-averaged techniques like X-ray magnetic circular dichroism[24, 26] for the characterization of magnetic properties.

Acknowledgement:

The authors are greatly indebted to Jens Brede for insightful discussions and technical assistance in experimental measurements, and Nicolae Atodiresei for helpful discussions. This work is funded by the DFG via SFB668-A5 and SFB/TRR 88 3MET, the EU via the ERC Advanced Grant FURORE, the Hamburgische Stiftung für Wissenschaft und Forschung via the Cluster of Excellence NANOSPINTRONICS, and the NSF-OISE 0730257 via the SPIRE project.

Supporting information Available:

Additional STM images show the chirality of 4-lobed $TbPc_2$ molecules on the Ir(111) surface with different orientations, the threshold switching bias of $TbPc_2$ against tip-sample separations from the chiral to the achiral state, and $TbPc_2$ molecules all exhibiting 8-lobed structures after a low temperature molecule deposition.

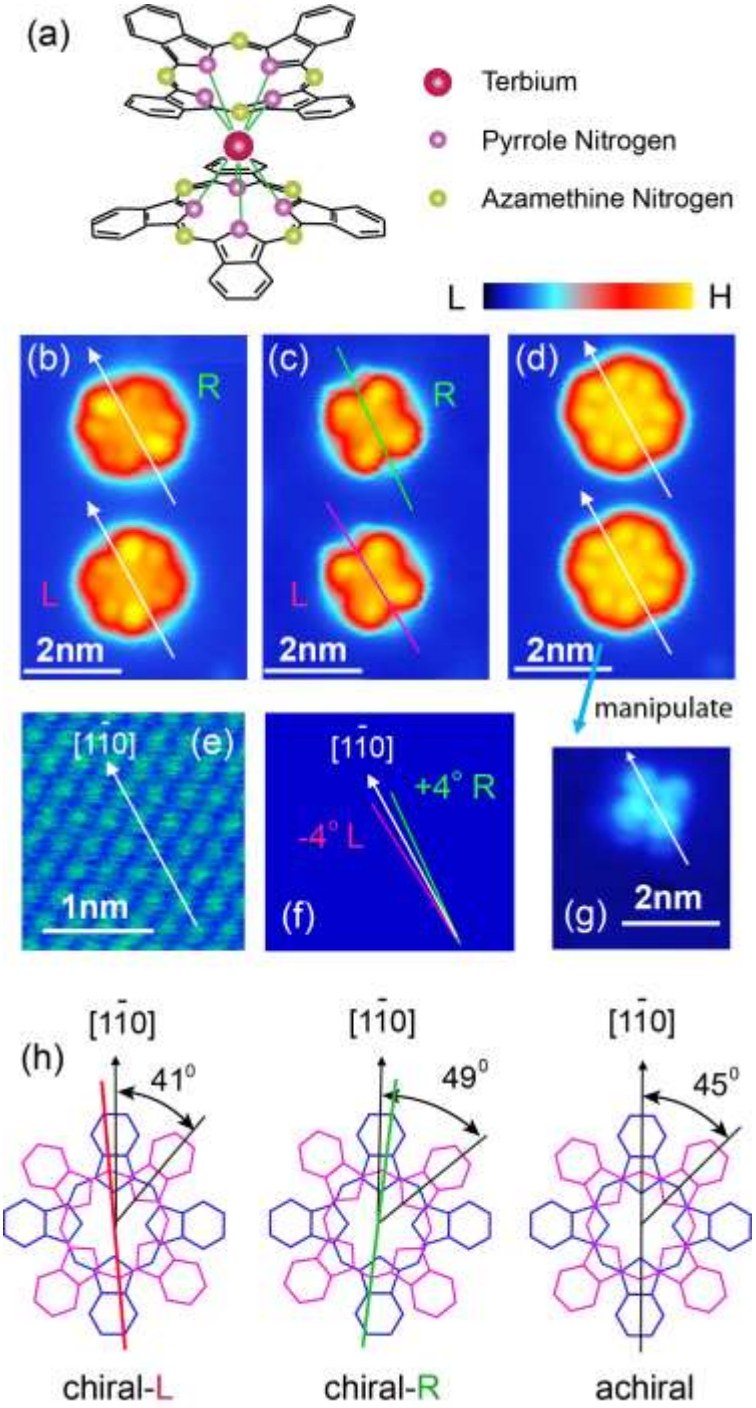

Figure 1. Chirality of $TbPc_2$ on Ir(111). (a) Molecular structure of $TbPc_2$. (b-d) STM images show two $TbPc_2$ molecules which are initially chiral (b, c), and become achiral in an 8-lobed state (d) after switching. Imaging conditions: V = -1.0 V, I = 0.1 nA for (c); V = 1.7 V, I = 0.1 nA for (b) and (d). The principal axis of the L/R chiral $TbPc_2$ (red/green line) indicates a misalignment of –/+ 4° with respect to the [1-10] direction (white arrow) of Ir(111), as is depicted in (f). The principal axis of the 8-lobed $TbPc_2$ in (d) aligns with [1-10]. (e) Atomic resolution of Ir(111) (-1.0V, 0.2nA) with [1-10] direction labeled. (g) STM image (-1.0V, 0.2nA) of a single-decker decomposed from an identically oriented $TbPc_2$ as in (d) with a lateral tip manipulation (0.3 V, 50 nA) along the light blue arrow direction. (h) Structural models of $TbPc_2$ with different chirality properties corresponding to their adsorption configurations in (b-d). The lower Pc (colored in blue) has two opposite lobes along [1-10]. The principal axis of the upper Pc (colored in purple) is marked with a red/green line for the left/right-handed $TbPc_2$. The staggering angles between the two Pcs are indicated.

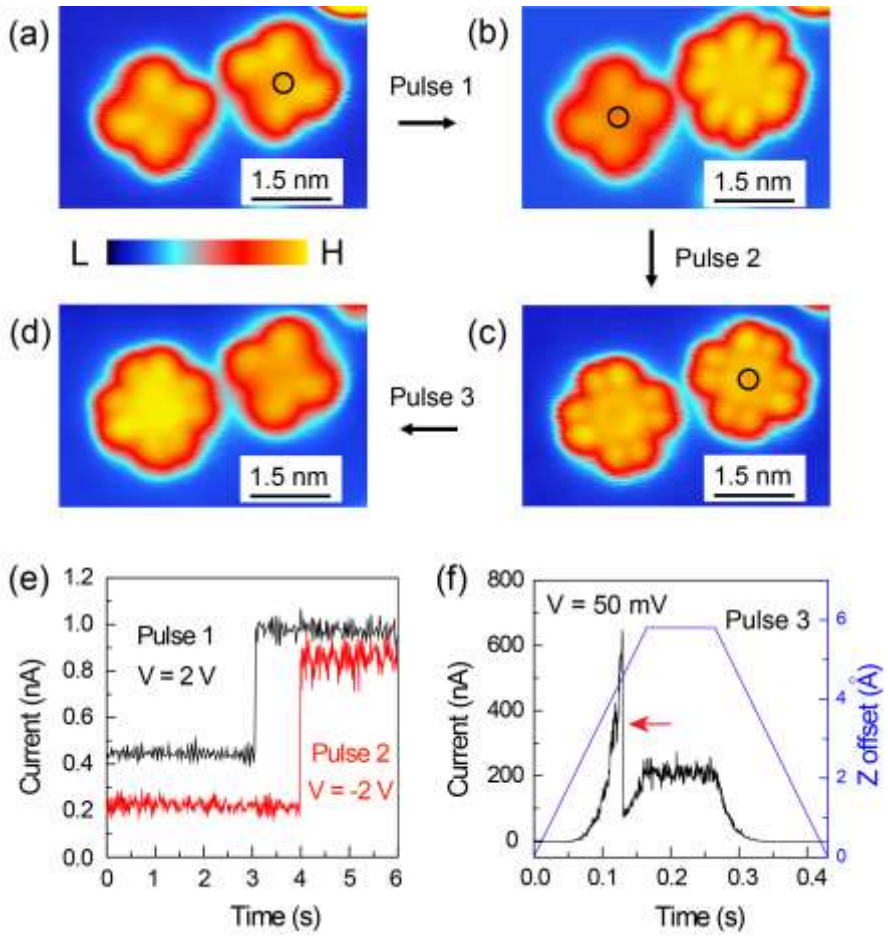

Figure 2. Reversible switching of $TbPc_2$ on Ir(111). (a-d) A sequence of STM images showing the controlled switching of $TbPc_2$ molecules between a chiral 4-lobed state and an achiral 8-lobed state on Ir(111). Each consecutive image shows the outcome of the STM tip manipulations whose position is marked in the previous image with a circle. Imaging conditions: -1.0 V, 0.1 nA. (e, f) Tunneling current recorded over time during the switching manipulations with the tip positioned above the center of the molecule. The feedback loop was stabilized at 1.0 V, 0.1 nA (-1.0 V, 0.1 nA) prior to and opened during manipulations with a voltage pulse of 2 V (-2 V) for Pulse 1 (2). In (f), the feedback loop was stabilized at -1.0 V, 0.1 nA prior to and opened during the manipulation which was performed with controlled tip movement and a constant applied voltage of 50 mV. A red arrow marks an abrupt current change associated with the molecule switching from the achiral to the chiral state.

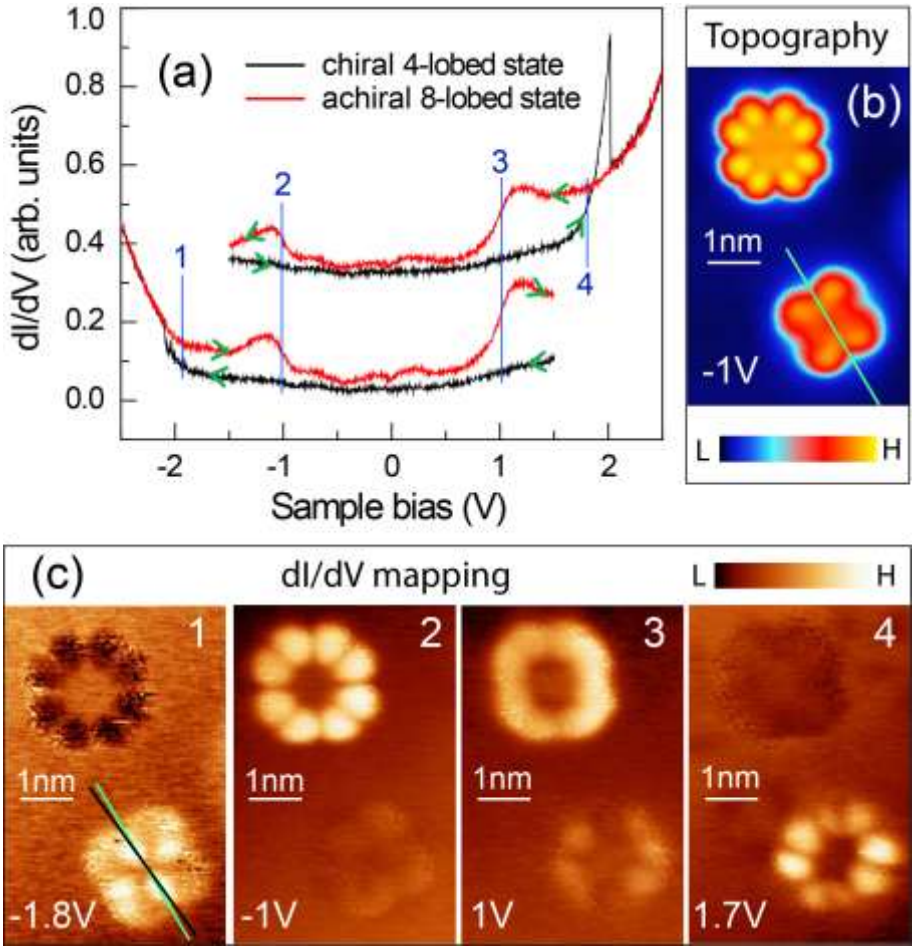

Figure 3. Electronic structure of $TbPc_2$ on Ir(111). (a) Differential conductance spectra measured above the center of $TbPc_2$. The bias ramping directions are marked with green arrows. The molecules were originally in the chiral 4-lobed state, and the abrupt conductance changes indicate the switching transitions to the achiral 8-lobed state. (Tunneling gap: -1.0 V, 0.1 nA. Modulation voltage: 20 mV.) The numbers labeled in (a) correspond to the numbering in (c). (b) Topographic image (-1.0 V) of two $TbPc_2$ molecules in different states. (c) Conductance mapping of the two molecules in (b) taken at as indicated bias voltages, showing the spatial distributions of their frontier orbitals both in the chiral state (mapping 1 and 4) and in the achiral state (mapping 2 and 3). The principal axis of the chiral molecule's upper/lower Pc is marked with a green/black line in (b) and mapping 1 of (c). The STM images and mappings were obtained in constant current mode at 0.1 nA with a modulation of 30 mV.

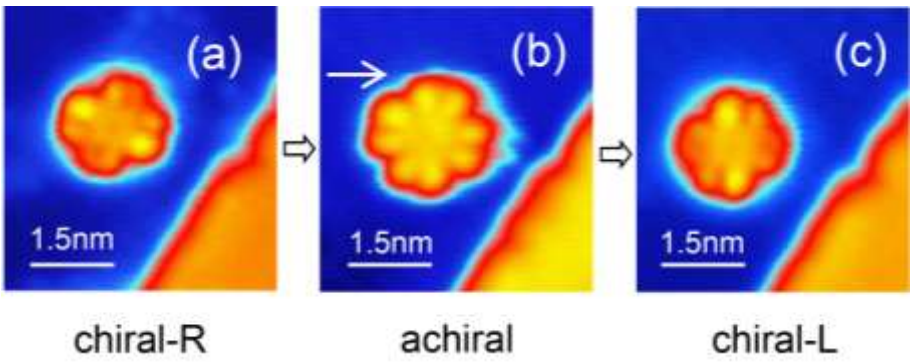

Figure 4. Chirality manipulation of $TbPc_2$ on Ir(111). STM topographic images of a $TbPc_2$ molecule switched from the chiral state (a) to the achiral state (b) and further switched back (c). A white arrow in (b) marks the switching during scanning, where the slow scanning direction is from top to bottom. Chirality properties of the respective switching states are indicated below the corresponding STM images. Imaging parameters: V = 1.7 V, I = 0.1 nA for (a) and (c); V = -2.5 V, I = 0.1 nA for (b).

References:

1. Molen, S. J.; Liljeroth, P. *J. Phys.: Condens. Matter* **2010**, 22, 133001.

2. Qiu, X. H.; Nazin, G. V.; Ho, W. *Phys. Rev. Lett.* **2004**, 93, 196806.

3. Liljeroth, P.; Repp, J.; Meyer, G. *Science* **2007**, 317, 1203.

4. Henzl, J.; Mehlhorn, M.; Gawronski, H.; Rieder, K. H.; Morgenstern, K. *Angew. Chem. Int. Ed.* **2006**, 45, 603.

5. Choi, B. Y.; Kahng, S. J.; Kim, S.; Kim, H.; Kim, H. W.; Song Y. J.; Ihm, J.; Kuk, Y. *Phys. Rev. Lett.* **2006**, 96, 156106.

6. Wang, Y. F.; Kröger, J.; Berndt, R.; Hofer, W. A. *J. Am. Chem. Soc.* **2009**, 131, 3639.

7. Comstock, M. J.; Strubbe, D. A.; Berbil-Bautista, L.; Levy, N.; Cho, J.; Poulsen, D.; Fréchet, J. M. J.; Louie, S. G.; Crommie, M. F. *Phys. Rev. Lett.* **2010**, 104, 178301.

8. Iancu, V.; Hla, S. W. *Proc. Nat. Acad. Sci.* **2006,** 103, 13718.

9. Pavliček, N.; Fleury, B.; Neu, M.; Niedenführ, J.; Herranz-Lancho C.; Ruben, M.; Repp, J. *Phys. Rev. Lett.* **2012**, 108, 086101.

10. Auwärter, W.; Seufert, K.; Bischoff, F.; Ecija, D.; Vijayaraghavan, S.; Joshi, S.; Klappenberger, F.; Samudrala, N.; Barth, J. V. *Nat. Nanotech.* **2012**, 7, 41.

11. Leoni, T.; Guillermet, O.; Walch, H.; Langlais, V.; Scheuermann, A.; Bonvoisin, J.; Gauthier, S. *Phys. Rev. Lett.* **2011**, 106, 216103.

12. Wu, S. W.; Ogawa, N.; Ho, W. *Science* **2006**, 312, 1362.

13. Fu, Y. S.; Zhang, T.; Ji, S. H.; Chen, X.; Ma, X. C.; Jia, J. F.; Xue, Q. K. *Phys. Rev. Lett.* **2009**, 103, 257202.

14. Swart, I.; Sonnleitner, T.; Repp, J. *Nano Lett.* **2011**, 11, 1580.

15. Mohn, F.; Repp, J.; Gross, L; Meyer, G; Dyer, M. S.; Persson, M. *Phys. Rev. Lett.* **2010**, 105, 266102.

16. Ernst K. H. *Top. Curr. Chem.* **2006**, 265, 209.

17. Barlow, S.M.; Raval, R. *Surf. Sci. Rep.* **2003**, 50, 201.

18. Parschau, M.; Passerone, D.; Rieder K. H.; Hug, H. J.; Ernst, K. H. *Angew. Chem. Int. Ed.* **2009**, 48, 4065.

19. Simic-Milosevic, V.; Meyer J.; Morgenstern, K. *Angew. Chem. Int. Ed.* **2009**, 48, 4061.

20. Qi, D.D.; Zhang, L.J.; Wan, L.; Zhang, Y.X.; Bian, Y.Z.; Jiang, J.Z. *Phys. Chem. Chem. Phys.*, **2011**, 13, 13277.

21. Ishikawa, N.; Sugita. M.; Ishikawa, T.; Koshihara, S.; Kaizu, Y. *J. Am. Chem. Soc.* **2003**, 125, 8694.

22. Vitali, L.; Fabris. S.; Conte, A. M. ; Brink. S. ; Ruben. M. ; Baroni, S ; Kern, K. *Nano Lett.* **2008**, 8, 3364.

23. Zhang, Y. F.; Isshiki. H; Katoh, K.; Yoshida, Y; Yamashita, M.; Miyasaka, H; Breedlove, B. K.; Kajiwara, T.; Takaishi, S.; Komeda. T. *J. Phys. Chem. C* **2009**, 113, 9826.

24. Gonidec, M.; Biagi, R.; Corradini, V.; Moro, F.; De Renzi, V.; del Pennino, U.; Summa, D.; Muccioli, L.; Zannoni, C.; Amabilino, D.B.; Veciana, J. *J. Am. Chem. Soc.*, **2011**, 133, 6603.

25. Komeda, T.; Isshiki, H.; Liu, J.; Zhang, Y. F.; Lorente, N.; Katoh, K.; Breedlove, B. K.; Yamashita, M. *Nat. Commun.* **2011**, 2, 217.

26. Lodi Rizzini, A.; Krull, C.; Balashov, T.; Kavich, J. J.; Mugarza, A.; Miedema, P. S.;

Thakur, P. K.; Sessi, V.; Klyatskaya, S.; Ruben, M.; Stepanow, S.; Gambardella, P. *Phys. Rev. Lett.* **2011**, 107, 177205.

27. Urdampilleta, M.; Klyatskaya, S.; Cleuziou, J. P.; Ruben, M.; Wernsdorfer, W. *Nat. Mater.* **2011**, 10, 502.

28. Wittneven, Ch.; Dombrowski, R.; Pan, S. H.; Wiesendanger, R. *Rev. Sci. Instr.* **1997**, 68, 3806.

29. Fu, Y. S.; Ji, S. H.; Chen, X.; Ma, X.C.; Wu, R.; Wang, C. C.; Duan, W. H.; Qiu, X. H.; Sun, B.; Zhang, P.; Jia, J. F.; Xue, Q. K. *Phys. Rev. Lett.* **2007**, 99, 256601.

30. Otsuki, J.; Komatsu, Y.; Kobayashi, D.; Asakawa, M.; Miyake, K. *J. Am. Chem. Soc.* **2010**, 132, 6870.

31. Écija, D.; Auwärter, W.; Vijayaraghavan, S.; Seufert, K.; Bischoff, F.; Tashiro, K.; Barth, J. V. *Angew. Chem. Int. Ed.* **2011**, 50, 3872.

32. A helical twist between the two Pc rings of the 4-lobed molecule could possibly happen, as the Coulomb repulsion between them becomes asymmetric after the 4° azimuthal rotation.

33. We have also investigated $DyPc_2$ molecules on the same substrate, which show the same switching behavior with no discernible features to $TbPc_2$. This further substantiates the assignment of switching to the dynamics of *bis*-Pc ligands.

34. Stipe, B. C.; Rezaei, M. A.; Ho, W.; Gao, S.; Persson, M.; Lundqvisit, B. I. *Phys. Rev. Lett.* **1997**, 78, 4410.

35. In view of the short time scale (0.45 s) of the pulse, the STM piezo tube suffers from a relaxation effect. Therefore, the applied Z offset value is larger than the actual value for achieving a desired tunneling current.

36. Schulze, G.; Franke, K. J.; Gagliardi, A.; Romano, G.; Lin, C. S.; Rosa, A. L.; Niehaus, T.

A.; Frauenheim, Th.; Di Carlo, A.; Pecchia, A.; Pascual, J. I. *Phys. Rev. Lett.* **2008**, 100, 136801.

37. We cannot rule out the possibility of switching due to the perturbation of the tip in close-proximity to the molecule during the reverse switching manipulation.

38. In a topography corrected image only two of these four lobes appear pronounced, maintaining the orientation discussed here.

39. Wiesendanger, R. *Rev. Mod. Phys.* **2009**, 81, 1495.